VHL and PTEN loss coordinate to promote mouse liver vascular lesions

Shufen Chen,
Lineberger Comprehensive Cancer Center, University of North Carolina at Chapel Hill, Campus Box 7295, Room 21-237, Chapel Hill, NC 27599-7295, USA

Christie A. Sanford,
Lineberger Comprehensive Cancer Center, University of North Carolina at Chapel Hill, Campus Box 7295, Room 21-237, Chapel Hill, NC 27599-7295, USA

Junjiang Sun,
Gene Therapy Center, University of North Carolina at Chapel Hill, Chapel Hill, NC 27599, USA

Vivian Choi,
Gene Therapy Center, University of North Carolina at Chapel Hill, Chapel Hill, NC 27599, USA

Terry Van Dyke,
Lineberger Comprehensive Cancer Center, University of North Carolina at Chapel Hill, Campus Box 7295, Room 21-237, Chapel Hill, NC 27599-7295, USA

R. Jude Samulski, and
Lineberger Comprehensive Cancer Center, University of North Carolina at Chapel Hill, Campus Box 7295, Room 21-237, Chapel Hill, NC 27599-7295, USA

Gene Therapy Center, University of North Carolina at Chapel Hill, Chapel Hill, NC 27599, USA

W. Kimryn Rathmell
Lineberger Comprehensive Cancer Center, University of North Carolina at Chapel Hill, Campus Box 7295, Room 21-237, Chapel Hill, NC 27599-7295, USA

Abstract

Von Hippel-Lindau (*VHL*) inactivation develops a tumor syndrome characterized by highly vascularized tumors as a result of hypoxia inducible factors (HIF) stabilization. The most common manifestation is the development of hemangioblastomas typically located in the central nervous system and other organs including the liver. *PTEN* (Phosphatase and tension homologue deleted on chromosome 10) inactivation also upregulates HIF-1α and may take part in promoting vascular lesions in tumors. The coordinate effect of loss of these tumor suppressors on HIF levels, and the subsequent effect on vascular lesion formation would elucidate the potential for mechanisms to modify HIF dosage supplementally and impact tumor phenotype. We therefore employed models of somatic conditional inactivation of *Vhl, Pten*, or both tumor suppressor genes in individual cells of the liver by Cre-loxP recombination to study the cooperativity of these two tumor suppressors in preventing tumor formation. Nine months after tumor suppressor inactivation, *Vhl* conditional deletion (*Vhl*$^{loxP/loxP}$) mice showed no abnormalities, *Pten* conditional deletion (*Pten*$^{loxP/loxP}$) mice developed liver steatosis and focal nodular expansion of hepatocytes containing lipid droplet and fat. *Vhl* and *Pten* conditional deletion (*Vhl*$^{loxP/loxP}$; *Pten*$^{loxP/loxP}$) mice, however, developed multiple cavernous liver lesions reminiscent of hemangioblastoma. Liver hemangioblastomas in VHL disease

may, therefore, require secondary mutation in addition to *VHL* loss of heterozygosity which is permissive for vascular lesion development or augments levels of HIF-1α.

Keywords

Von Hippel-Lindau (VHL); Phosphatase and tension homologue deleted on chromosome 10 (PTEN); Adeno associated virus (AAV); Cre recombination; Gene therapy; Liver hemangioma

Introduction

Von Hippel-Lindau (VHL) syndrome is an autosomal dominant multi-system disorder characterized by abnormal growth of blood vessels and angiogenic tumors. The most common manifestation is hemangioblastomas typically located in the central nervous system and other organs including liver [1,2]. VHL syndrome is caused by mutation of *VHL* gene on the short arm of the third chromosome (3p25). Most patients with VHL disease inherit one mutant copy of *VHL* gene from one parent and somatically lose the wild type allele, consistent with the tumor suppressor gene "two hit hypothesis" [3]. Somatic *VHL* loss contributes to the development of sporadic cancers as well, in particular clear cell type renal cell carcinoma [4, 5]. *VHL* loss contributes to tumorigenicity by permitting the post-translational stabilization of the hypoxia inducible factors (HIF-1α and HIF-2α) [6]. The HIF factors facilitate the transcription of a wide repertoire of hypoxia response genes which promote angiogenesis and tumor growth.

Phosphatase and tension homologue deleted on chromosome 10 (*PTEN*), a tumor suppressor gene in a variety of tumors, is implicated in the familial Cowden syndrome [7]. Its inactivation permits activation of AKT (also known as protein kinase B, PKB) phosphorylation and subsequent induction of downstream HIF-1α protein translation and may take part in angiogenesis and vascular lesions in tumors. Additionally, loss of *PTEN* has been shown to play a role in increasing the transcriptional activation induced by HIF-1α by a mechanism that is independent of AKT phosphorylation [8].

It is not known whether these distinct mechanisms of HIF regulation operate only as parallel means to achieve the same HIF response, or if the degree of HIF activation can be modulated and have potential to impact tumor phenotype. Within the context of *VHL* mutation, we have observed a graded effect of HIF disregulation with missense mutations as compared to the null allele [9,10]. The combined loss of *VHL* and *PTEN* is observed in some tumors, suggesting that there may be non-overlapping roles of these two tumor suppressors in modulating tumorigenesis. We therefore sought to understand if effects of *PTEN* loss on HIF regulation and activity could enhance the already increased levels of HIF in a *VHL* null setting.

Mice homozygous for the *Vhl* null allele are lethal at embryonic midgestation due to placenta vascular abnormalities [11]. To circumvent the embryo's lethality of *Vhl* gene knockout, mice carrying a loxP-flanked *Vhl* allele (*Vhl*^loxP/loxP^) were generated and the Cre-loxP technique was used to conditionally inactivate *Vhl* gene [12]. Although several research groups have generated mouse and tissue specific mice models using conditional *Vhl* inactivation, *Vhl* somatic loss and the subsequent effects on lesion formation or tumorigenesis have not been examined [12–15].

In order to investigate the cumulative effect of postnatal somatic *Vhl* and *Pten* loss on HIF expression and the development of vascular lesions, we developed a modified self-complementary Adeno-associated virus carrying Cre recombinase (scAAV-Cre) [16,17]. The vector was introduced by tail vein injection into adult mice with one of a panel of conditional

tumor suppressor gene knockout backgrounds: *Vhl* allele (*Vhl*$^{loxP/loxP}$), *Pten* allele (*Pten*$^{loxP/loxP}$), or both *Vhl* and *Pten* alleles (*Vhl*$^{loxP/loxP}$;*Pten*$^{loxP/loxP}$). Loss of either tumor suppressor alone gave a mild, but distinct phenotype, however, *Vhl*$^{loxP/loxP}$;*Pten*$^{loxP/loxP}$ mice developed multiple cavernous vascular liver lesions reminiscent of hemangioblastoma. HIF-1α and HIF-2α levels were highly upregulated in these vascular lesions, although they were barely detectable throughout the liver of mice conditional loss of only one tumor suppressor *Vhl* or *Pten*. This model demonstrates that dual strategies to engage pro-angiogenic pathways can be additive and engage mutually permissive environments for angiogenic lesion formation.

Materials and methods

AAV viral vectors

A recently constructed AAV2 vector plasmid, pHpa-Trs-SK [16,17], was used to produce the self-complementary AAV2 viral vector (scAAV-GFP) containing a human cytomegalovirus (CMV) promoter and an enhanced GFP gene (Fig. 1a). This construct packages only dimeric inverted repeat genomes. The scAAV-Cre vector plasmid carrying Cre recombinase was constructed from pHpa-Trs-SK. First, GFP was removed from pHpa-Trs-SK plasmid by digesting with AgeI and NotI. Then, 1,032 bp of the Cre cassette was amplified from the plasmid pCAAGS-Cre [18] by PCR, using the following primers: 5′Cre XmaI (5′-ATC CCC CCG GGA TGT CCA ATT TAC TGA CCG TA-3′) and 3′Cre NotI (5′-ATA AGA ATG CGG CCG CCT AAT CGC CAT CTT CCA-3′). XmaI and NotI restriction enzyme sites were added to the 5′ and 3′ ends, respectively during the PCR. This fragment was inserted into the pHpa-Trs-SK vector with the Rapid DNA Ligation Kit (Roche, Basel, Switzerland). The structure of the scAAV-Cre plasmid (Fig. 1b) was confirmed by restriction digestion and sequence analysis performed by the Automated DNA Sequencing Facility at the University of North Carolina at Chapel Hill. The recombinant AAV viral vectors used in this study were prepared in 293T cells using three-plasmid co-transfection, and purified following previously published methods [19] by the Vector Core Facility, Gene Therapy Center, University of North Carolina at Chapel Hill.

Mouse genetics and in vivo administration of vectors

All mice used in this study were bred and maintained in the Laboratory Animal Facility of University of North Carolina at Chapel Hill using protocols approved by the UNC institutional animal care and use committee. ROSA26 lox-stop-lox-LacZ reporter mice (Jackson Laboratories, Bar Harbor, ME) [20] and C57BL/6 mice with a loxP-flanked *Pten* allele (*Pten*$^{loxP/loxP}$) were kindly provided by Dr. T. Van Dyke [21]. BALB/c mice with a loxP-flanked *Vhl* allele (*VHL*$^{loxP/loxP}$) were kindly provided by Dr. Volker Haase [12]. *Vhl*$^{loxP/loxP}$ mice were intercrossed with *Pten*$^{loxP/loxP}$ mice to generate *Vhl*$^{loxP/wt (wildtype)}$;*Pten*$^{loxP/wt}$ mice. These *Vhl*$^{loxP/wt}$;*Pten*$^{loxP/wt}$ mice were subsequently intercrossed to generate *Vhl*$^{loxP/loxP}$;*Pten*$^{loxP/loxP}$ mice, which were mixed genetic background (BALB/c, C57BL/6), littermates were used as controls.

ROSA26 lox-stop-lox-LacZ reporter mice were intravenously (I.V.) injected with a total of 10^{11} particles of scAAV empty capsid, or scAAV-GFP or scAAV-Cre vector in a final volume of 100 μl with a 30-gauge needle via tail vein. The ROSA26 reporter mice were sacrificed at 4 weeks after the injection and organs including liver, kidney, spleen, heart, and lung were harvested for analysis of reporter gene expression.

Vhl$^{loxP/loxP}$, *Pten*$^{loxP/loxP}$, *Vhl*$^{loxP/loxP}$;*Pten*$^{loxP/loxP}$ mice or control littermates were injected via the tail vein with 10^{11} particles of scAAV empty vector, or scAAV-Cre vector in a final

volume of 100 μl at the age of 6 weeks. Animals were euthanized at a time point 9 months after the injection and autopsied for phenotype evaluation.

The $Vhl^{loxP/wt}$ alleles were detected by PCR amplification of the loxP site, yielding 400 and 200 bp products for the floxed and wildtype alleles, respectively using the primers: Vhl forward 1 (5′-CCG GAG TAG GAT AAG TCA GCT GAG-3′) and Vhl reverse (5′-CTG ACT TCC ACT GAT GCT TGT CAC AG-3′). The PCR condition was 94°C for 10 min (min), 35 cycles of 94°C 50 s, 58°C 50 s, and 72°C 1 min, and 72°C 5 min extension. Detection of $Pten^{loxP/wt}$ alleles yielded 435 and 310 bp products for the floxed and wildtype alleles using the primers: $Pten$ forward (5′-TGT TTT TGA CCA ATT AAA GTA GGC TGT G-3′) and $Pten$ reverse (5′-AAA AGT TCC CCT GCT GAT GAT TTG T-3′). The PCR condition was 94°C for 2 min, 34 cycles of 94°C 20 s, 62°C 45 s, and 72°C 45 s, and 72°C 2 min extension. Products were resolved in 1.5% agarose gels and visualized with ethidium bromide under UV light.

PCR analysis of recombination

Microdissection of hemangiomas was performed using a laser capture microdissection (LCM) system. 4 μm sections from formalin fixed and paraffin embedded tissue were used after dewaxing in xylene and drying. The dissected tissue was transferred into 25 μl of proteinase K buffer and incubated with proteinase K at 56°C overnight, followed by inactivation of proteinase K at 95°C for 10 min. 5 μl was used for subsequent PCR to detect recombined Vhl using the following primers: forward 2 (5′-CTG GTA CCC ACG AAA GTG TC-3′) and Vhl reverse (5′-CTG ACT TCC ACT GAT GCT TGT CAC AG-3′) yielding a 250 bp product for the recombined Vhl allele (Fig. 3d) [12]. For the detection of recombined $Pten$, the following primers were used for PCR: primer 1 (5′-AAA AGT TCC CCT GCT GAT GAT TTG T-3′) and primer 2 (5′-TTC CTT AGC CTG TTC AG C-3′), which yielded an around 1 kb product for the recombined $Pten$ allele (Fig. 3e) [21].

Assays of reporter gene expression

To detect the expression of GFP, organs harvested from the scAAV-GFP vector injected mice were embedded in Optional Cutting Temperature (OCT, Electron Microscopy Sciences, Hatfield, PA), snap frozen, and sectioned on a cryostat (10 μm sections). Sections were examined for GFP expression using a fluorescence microscope with a fluorescein filter set.

To examine the β-galactosidase expression, livers from the scAAV-Cre injected ROSA26 reporter mice were harvested, some tissue fixed in 10% formalin overnight, dehydrated in gradient ethanol, embedded in paraffin, sectioned, and stained with hematoxylin and eosin (HE), while other liver tissue was snap frozen and embedded in OCT for frozen sections, which were stained using an X-gal staining kit pH 8.5, according to manufacturer's instructions (Chemicon International, Temecula, CA). Sections were counterstained with eosin prior to dehydration through gradient ethanol and xylene and were mounted using Cytoseal™ XYL (Richard-Allan Scientific, Kalamazoo, MI).

Histological analysis and immunohistochemistry

The organs harvested from $Vhl^{loxP/loxP}$, $Pten^{loxP/loxP}$, and $Vhl^{loxP/loxP};Pten^{loxP/loxP}$ mice were fixed in 10% formalin overnight, dehydrated in gradient ethanol, and embedded in paraffin. 4 μm sections were cut and stained with hematoxylin and eosin (HE) and Periodic Acid-Schiff (PAS). Some harvested livers were snap frozen, embedded in OCT, sectioned on a cryostat, and stained with oil red O.

Immunohistochemistry staining was performed on formalin fixed paraffin embedded sections according to the protocol from Vector ABC Elite Kit. Antigen retrieval for all antibodies was

done by boiling the slides in citrate buffer (pH 6.0; BioGenex) for 30 min. Endogenous peroxidase activity was quenched in 3% H_2O_2 for 10 min. Antibodies used were: anti-HIF-1α (Clone H1 alpha 67, mouse monoclonal antibody, 1:50, Novus), anti-HIF-2α (Clone 190b, mouse monoclonal antibody, 1:100, Gene-Tex), anti-Ki67 (Clone SP6, rabbit polyclonal antibody, 1:200, Lab Vision Corporation), anti-phosphorylated AKT (p-AKT, Ser 473, 1:200, Cell Signaling), anti-vascular epithelial growth factor (VEGF, A-20, SC-152, rabbit polyclonal antibody, 1:100, Santa Cruz), and anti-platelet endothelial cell adhesion molecule 1 (PECAM, CD31, rabbit polyclonal antibody, 1:50, Abcam). Detection for all antibodies was performed using the Vector ABC Elite Kit and a Vector DAB kit for substrate detection (Vector Labs, Burlingame, CA). Immunofluorescence detection followed the same protocol, except that signal amplification used TSA Plus Fluorescence System (Perkin-Elmer, Wellesley, MA) and slides were mounted with Vectashield Vector mount media (Vector Laboratories). Digital images were captured with a Nikon DMX-1200 color digital camera using the ACT-1 software (Nikon, Melville, NY).

Results

Intravenous gene delivery and recombination with scAAV

The scAAV viral system was developed to permit the induction of cre recombination in the liver without invoking an immune response. Further, as the effect of gene loss on single cells in an otherwise unperturbed environment was desired, a virus affecting a limited percentage of cells in the liver was selected. To examine the effectiveness of scAAV transduction in the liver and the stability of virally expressed proteins, the scAAV-GFP vector was injected into mice via tail vein. The mice were euthanized 4 weeks after the injection and organs were harvested, frozen, sectioned, and examined for the persistent expression of the GFP transgene by fluorescence microscopy. At the dosage injected, GFP expression was visible in scattered cells in the liver, transfecting around 20–30% of hepatocytes, but not in other organs (Fig. 1c and data not shown). No GFP expression was observed in AAV2 empty capsid injected control animals.

The scAAV vector system was modified to deliver Cre recombinase in order to expand the potential for tissue specific transgenic induction. In order to visually evaluate the areas of recombination, ROSA26 lox-stop-lox-LacZ reporter mice were subjected to in vivo delivery of the scAAV-Cre vector. Organs were harvested and β-galactosidase staining was performed at 4 weeks after the scAAV-Cre injection (Fig. 1d). The Cre-dependent recombination event, monitored by β-galactosidase-positive staining, was observed in liver (Fig. 1d). Positive cells were observed quite widely dispersed and around 30% hepatocytes were infected in the liver. No LacZ activity was detected in other organs such as kidney, spleen, heart, and lung (data not shown). There was no inflammatory cell infiltration in liver and other organs indicating no immune response to the vector (Fig. 1e and data not shown).

Vhl and *Pten* loss cooperates to promote the development of vascular lesions

scAAV-Cre vector was injected into *Vhl*$^{loxP/loxP}$, *Pten*$^{loxP/loxP}$, and *Vhl*$^{loxP/loxP}$; *Pten*$^{loxP/loxP}$ mice via tail vein to investigate the potential for coordinate effects of inactivation of the tumor suppressor genes *Vhl* and *Pten*. Grossly, the livers of *Vhl*$^{loxP/loxP}$ or *Pten*$^{loxP/loxP}$ mice displayed no visible abnormalities at 4, 9, and 12 months after the AAV-Cre vector injection. However, *Vhl*$^{loxP/loxP}$;*Pten*$^{loxP/loxP}$ mice displayed large discrete lesions visible both on the surface of the liver and within the liver parenchyma by 9 months after the AAV-Cre vector injection (Fig. 2a–c). These gross anatomic lesions were only associated with combined loss of *Vhl* and *Pten*.

Histologically, conditional *Vhl* loss showed minimal abnormalities in liver (Fig. 2d, g), which differed from prior studies with albumin-cre directed excision [12]. *Pten* loss, however, produced a high penetrance of discrete liver nodules with disorganized cellular architecture, and cells which displayed a vacuolated cytoplasm, surrounded by normal appearing hepatic parenchyma. The edge of one such nodule is depicted in Fig. 2e, h. Additionally, hepatic nodules displaying cells with marked atypia and basophilic cytoplasm were observed in a subset of these animals (data not shown). When the genetic events were combined, histologic examination of livers from $Vhl^{loxP/loxP}$;$Pten^{loxP/loxP}$ mice sacrificed 9 months after scAAV-Cre vector administration detected expansile, highly vascular lesions with a complex cellular architecture (Fig. 2f, i), in which some small blood vessels showed PECAM positive further demonstrating angiogenesis may happen (Fig. 8c). None of the lesions associated with the individual loss of *Vhl* or *Pten* were observed, as shown in Table 1, a summary of the findings associated with each genotype was provided. These discrete vascular lesions corresponded to the grossly visible nodules in the liver, and shared features of liver hemangioblastoma, although at 9 months there was no evidence of local invasion or metastatic spread.

Hepatic vascular lesions show evidence of *Vhl* and *Pten* loss

PCR analysis of microdissected liver tissue from the highly vascular lesions associated with the $Vhl^{loxP/loxP}$;$Pten^{loxP/loxP}$ genotype showed that the expected target *Vhl* and/or *Pten* alleles were recombined and deleted, as indicated by recombination of the *Vhl* or *Pten* locus. A representative PCR comparing the affected area of a highly vascular lesion with the expected PCR products from tail genotype of the mouse is shown (Fig. 3).

Vhl and *Pten* loss leads to distinct patterns of lipid accumulation

Conventional loss of *Vhl* is associated with a cellular conversion to anaerobic metabolism and an accumulation of cytoplasmic glycogen. In contrast, *Pten* loss, particularly in the liver, is associated with an accumulation of cytoplasmic lipid. The bioenergetic effects of the combined loss of these genes are unknown. Gross examination of the *Pten* mutant livers revealed hepatomegaly, and histological analysis demonstrated that the mutant hepatocytes within the nodules displayed large cytoplasmic vacuoles. A PAS stain for glycogen deposition was applied to the affected livers and demonstrated some areas of glycogen deposition in the $Vhl^{loxP/loxP}$ livers, but little extra accumulation was observed in the $Pten^{loxP/loxP}$ livers. However, less PAS staining was observed in the lesions present in $Vhl^{loxP/loxP}$;$Pten^{loxP/loxP}$ mice (Fig. 4a–c).

Similarly, oil red O was used to stain for lipid in these livers, demonstrating minimal lipid accumulation in the $Vhl^{loxP/loxP}$ mice. As expected, the nodules present in $Pten^{loxP/loxP}$ mice demonstrated marked accumulation of lipid, as did the highly vascular lesions of the $Vhl^{loxP/loxP}$;$Pten^{loxP/loxP}$ mice (Fig. 4d–f). Intense lipid uptake was not observed in other normal areas of the liver (data not shown).

Vhl and *Pten* loss additively affects cellular proliferation in livers of *Vhl* and *Pten* conditional deletion mice

The distinct lesions associated with each genetic profile, and in particular the appearance of nodule expansion, suggested that effects on cellular proliferation may be present. The proliferative nuclear marker Ki67 was utilized to detect dividing cells in liver lesions associated with each of the genotypes. Ki67 positive cells were significantly increased in the $Pten^{loxP/loxP}$ liver nodules as compared with the $Vhl^{loxP/loxP}$ lesions, and $Vhl^{loxP/loxP}$; $Pten^{loxP/loxP}$ livers displayed the most apparent increase in proliferation compared to either *Pten* or *Vhl* deleted alone (Fig. 5).

Upregulated phosphorylated AKT expression in hepatic lesion of *Vhl* and *Pten* conditional deletion mice

AKT is a downstream target of the PTEN regulated phosphatidylinositol 3 kinase (PI3K) pathway, its phosphorylation serving as an indicator of PTEN loss. We examined the localization of phosphorylated AKT using a phospho-specific immunofluorescence stain, which showed that cytoplasmic phosphorylated AKT expression was induced in hepatocytes in both the nodules of $Pten^{loxP/loxP}$ mice and the vascular lesions associated with $Vhl^{loxP/loxP};Pten^{loxP/loxP}$ mice (Fig. 6), verifying that upregulated phosphorylated AKT induced by *Pten* loss was a signaling mechanism activated in both of the genotype specific vascular lesions and fatty lesions.

Upregulated HIF-1α and HIF-2α expression in hepatic vascular lesions of *Vhl* and *Pten* conditional deletion mice

pVHL protein is involved in the ubiquitination and degradation of the transcription factor family members HIF-1α and HIF-2α. Loss of the pVhl protein results in stabilization of these proteins, and subsequent upregulation of hypoxia response target genes, which play important roles in regulating angiogenesis, cell growth, or cell survival [22]. In order to investigate the impact of *Vhl* inactivation on downstream HIF-1α and HIF-2α stabilization in the pathogenesis of vascular lesions in the $Vhl^{loxP/loxP};Pten^{loxP/loxP}$ conditional deletion mice, HIF-1α and HIF-2α were evaluated by immunofluorescence (Figs. 7, 8). In *Vhl* or *Pten* deletion mice, HIF-1α and HIF-2α were under the level of detection in the liver except in isolated cells, even in the presence of the genotype-specific lesions. Whereas the nuclear accumulation of both HIF-1α and HIF-2α in these lesions confirms the additive events activated by *Vhl* and *Pten* loss are present in this highly vascular lesions.

Upregulated PECAM and VEGF in hepatic vascular lesions of *Vhl* and *Pten* conditional deletion mice

In order to investigate the angiogenesis in *Vhl* and *Pten* conditional deletion mice, we stained the lesions for evidence of endothelial cell contribution with PECAM. In *Vhl* or *Pten* deletion mice, PECAM was sporadically positive throughout the liver and limited to the endothelial cells lining small vessels, whereas in *Vhl* and *Pten* conditional deletion mice, more PECAM positive cells were present in the lesions, demonstrating the contribution of cells with endothelial features to the overall mass (Fig. 9a–c).

VEGF is a downstream target of HIF-1 and HIF-2. In order to investigate the pathogenesis of the highly vascular lesions observed in *Vhl* and *Pten* conditional deletion mice, we stained the lesions for VEGF by immunohistochemistry. In *Vhl* or *Pten* single deletion mice, VEGF was sporadically positive in the liver, whereas in the liver vascular lesions of *Vhl* and *Pten* conditional deletion mice, there are more VEGF positive cells indicating that VEGF was coordinately expressed with HIF factors, and likely contributes to the vascular phenotype of the lesions as a result of HIF-1α and HIF-2α upregulation (Fig. 9d–f).

Discussion

The cooperative nature of concurrent loss of tumor suppressor genes raises many questions regarding the mechanisms which promote tumor progression. We have used an in vivo gene inactivation system to model the independent and concurrent loss of the tumor suppressors *Vhl* and *Pten*. Both are predicted to cause pro-angiogenic features of tumor development as a result of activation of HIF target genes, in the case of *Vhl* as a result of HIF stabilization, and in the case of *PTEN* as a result of AKT dependent increase in HIF protein translation, as well as an AKT-independent facilitation of HIF transcriptional activity. Whether quantitative effects on HIF levels or HIF activity specifically influence the degree of vascular lesion production,

or if HIF mediated effects occur as a result of surpassing a threshold of HIF activity, we have demonstrated that the combined loss of *Vhl* and *Pten* leads to a highly penetrant phenotype of expansile vascular lesion development in the liver.

We observed minimal pathological changes in the liver with *Vhl* loss alone, even after 1.5 years of latency following the AAV-Cre vector injection. This finding contrasts with that observed with either albumin or actin-cre induced *Vhl* recombination which promotes abundant loss of *Vhl* in the liver occurring at an early developmental time point [12,13]. Loss of *Vhl* function in single adult cells may be insufficient to induce lesion formation in the liver beyond rare simple liver hemangiomas, or further progression may require signals from neighboring affected cells. This model system is unique in restricting the genetic events to isolated cells within the adult liver parenchyma, thus excluding contributions from neighboring genetically modified cells or fields of genetically affected cells. Unique features of cellular organization in embryogenesis may also contribute to the different effects seen in our model system which is limited to adult animals. An alternate cause for these observations is that somatic abrupt loss of *Vhl* alone may trigger cellular senescence, as reported by Young et al. [23], thus accounting for the very minimal phenotype observed with *Vhl* loss alone.

Pten conditional deletion in our viral system consistently displayed the accumulation of round fatty nodules and hepatocyte vacuoles surrounded by regions of normal liver. Analysis for glycogen vs lipid accumulation in the lesions, confirmed that the *Pten* associated nodules display a phenotype of lipid accumulation. This is reminiscent of the fatty cell accumulation seen with widespread *Pten* loss in the liver, but suggests that the event of expansion of these hepatocytes has a clonal origin.

In contrast to the mild phenotypes of the single deletions, most (13/15, 86%) mice with combined inactivation of *Vhl* and *Pten* developed multiple macroscopically evident vascular lesions indicating that *Pten* and *Vhl* act as synergistically pro-angiogenic events in the liver lesion formation. Immunohistochemistry stain showed phosphor-ylated AKT upregulated in the cells lining liver lesions resembling hemangioblastomas, confirming that *Pten* loss in these lesions leads to the consequent constitutive activation of downstream components of the PI3K pathway known to drive angiogenesis via HIF-1α [24,25]. Therefore, *Pten* loss induced activated phosphorylated AKT combined with *Vhl* loss and the subsequent upregulated HIF pathway cooperated to induce highly vascular liver lesions not observed as a result of either event alone.

Both germline and somatic inactivation of the *VHL* tumor suppressor gene have been observed in hemangioblastomas and clear cell renal carcinomas [26]. The pVHL protein is involved in the ubiquitination and degradation of the transcription factors HIF-1α and HIF-2α, downstream of mTOR signaling [27]. Thus, the lesions may form as a result of supraphysiological levels of HIF-mediated signals, only sufficient with the combined loss of *Vhl* and *Pten* to promote the formation of these lesions. Alternative explanations exist, including the possibility that *Vhl* only acts as a tumor suppressor in the setting of a permissive environment and is not sufficient to produce a growth promoting phenotype. *Pten* loss may provide a supplementing genetic event, providing a proliferative signal to complement the physiology of *Vhl* loss, and the opportunity for *Vhl* to contribute to the development of a highly vascular phenotype. Hence, the AKT/mTOR signaling pathway, via activation of downstream HIF-1α regulatable genes or by presenting a permissive environment in which a *Vhl* lesion can be maintained, may play an integral role in the progression of VHL disease [28]. Future studies to determine whether other genetic events can fill this role to cooperate with *Vhl* loss to promote tumor formation are needed.

In summary, we have developed a mouse model resembling human liver hemangioblastomas by the combined conditional deletion of *Vhl* and *Pten*, which will be useful for understanding the additive pro-angiogenic events of the two tumor suppressor genes and screening anti angiogenesis drug treatments.

Acknowledgments

References

1. McGrath FP, et al. Case report: multiple hepatic and pulmonary haemangioblastomas—a new manifestation of von Hippel-Lindau disease. Clin Radiol 1992;45(1):37–39. [PubMed: 1740034]

2. Maher ER, Kaelin WG Jr. von Hippel-Lindau disease. Medicine (Baltimore) 1997;76(6):381–391. [PubMed: 9413424]

3. Chen F, et al. Suppression of growth of renal carcinoma cells by the von Hippel-Lindau tumor suppressor gene. Cancer Res 1995;55(21):4804–4807. [PubMed: 7585510]

4. Gnarra JR, et al. Mutations of the VHL tumour suppressor gene in renal carcinoma. Nat Genet 1994;7 (1):85–90. [PubMed: 7915601]

5. Shuin T, et al. Frequent somatic mutations and loss of heterozygosity of the von Hippel-Lindau tumor suppressor gene in primary human renal cell carcinomas. Cancer Res 1994;54(11):2852–2855. [PubMed: 8187067]

6. Rathmell WK, Simon MC. VHL: oxygen sensing and vasculogenesis. J Thromb Haemost 2005;3(12): 2627–2632. [PubMed: 15975138]

7. Brenner W, et al. Loss of tumor suppressor protein PTEN during renal carcinogenesis. Int J Cancer 2002;99(1):53–57. [PubMed: 11948491]

8. Emerling BM, et al. PTEN regulates p300-dependent hypoxia-inducible factor 1 transcriptional activity through Fork-head transcription factor 3a (FOXO3a). Proc Natl Acad Sci U S A 2008;105(7):2622– 2627. [PubMed: 18268343]

9. Rathmell WK, et al. In vitro and in vivo models analyzing von Hippel-Lindau disease-specific mutations. Cancer Res 2004;64(23):8595–8603. [PubMed: 15574766]

10. Lee CM, et al. VHL type 2B gene mutation moderates HIF dosage in vitro and in vivo. Oncogene 2009;28(14):1694–1705. [PubMed: 19252526]

11. Gnarra JR, et al. Defective placental vasculogenesis causes embryonic lethality in VHL-deficient mice. Proc Natl Acad Sci U S A 1997;94(17):9102–9107. [PubMed: 9256442]

12. Haase VH, et al. Vascular tumors in livers with targeted inactivation of the von Hippel-Lindau tumor suppressor. Proc Natl Acad Sci U S A 2001;98(4):1583–1588. [PubMed: 11171994]

13. Ma W, et al. Hepatic vascular tumors, angiectasis in multiple organs, and impaired spermatogenesis in mice with conditional inactivation of the VHL gene. Cancer Res 2003;63(17):5320–5328. [PubMed: 14500363]

14. Ding M, et al. Loss of the tumor suppressor Vhlh leads to upregulation of Cxcr4 and rapidly progressive glomerulonephritis in mice. Nat Med 2006;12(9):1081–1087. [PubMed: 16906157]

15. Frew IJ, et al. pVHL and PTEN tumour suppressor proteins cooperatively suppress kidney cyst formation. EMBO J 2008;27(12):1747–1757. [PubMed: 18497742]

16. McCarty DM, et al. Self-complementary recombinant adeno-associated virus (scAAV) vectors promote efficient transduction independently of DNA synthesis. Gene Ther 2001;8(16):1248–1254. [PubMed: 11509958]

17. McCarty DM, et al. Adeno-associated virus terminal repeat (TR) mutant generates self-complementary vectors to overcome the rate-limiting step to transduction in vivo. Gene Ther 2003;10 (26):2112–2118. [PubMed: 14625565]

18. Araki K, et al. Efficiency of recombination by Cre transient expression in embryonic stem cells: comparison of various promoters. J Biochem (Tokyo) 1997;122(5):977–982. [PubMed: 9443813]

19. Zolotukhin S, et al. Recombinant adeno-associated virus purification using novel methods improves infectious titer and yield. Gene Ther 1999;6(6):973–985. [PubMed: 10455399]

20. Takeda S, et al. Successful gene transfer using adeno-associated virus vectors into the kidney: comparison among adeno-associated virus serotype 1–5 vectors in vitro and in vivo. Nephron Exp Nephrol 2004;96(4):e119–e126. [PubMed: 15122061]

21. Chen Z, et al. Crucial role of p53-dependent cellular senescence in suppression of Pten-deficient tumorigenesis. Nature 2005;436(7051):725–730. [PubMed: 16079851]

22. Rathmell WK, Chen S. VHL inactivation in renal cell carcinoma: implications for diagnosis, prognosis and treatment. Expert Rev Anticancer Ther 2008;8(1):63–73. [PubMed: 18095884]

23. Young AP, et al. VHL loss actuates a HIF-independent senescence programme mediated by Rb and p400. Nat Cell Biol 2008;10(3):361–369. [PubMed: 18297059]

24. Di Cristofano A, Pandolfi PP. The multiple roles of PTEN in tumor suppression. Cell 2000;100(4): 387–390. [PubMed: 10693755]

25. Zundel W, et al. Loss of PTEN facilitates HIF-1-mediated gene expression. Genes Dev 2000;14(4): 391–396. [PubMed: 10691731]

26. Kim W, Kaelin WG Jr. The von Hippel-Lindau tumor suppressor protein: new insights into oxygen sensing and cancer. Curr Opin Genet Dev 2003;13(1):55–60. [PubMed: 12573436]

27. Inoki K, et al. Dysregulation of the TSC-mTOR pathway in human disease. Nat Genet 2005;37(1): 19–24. [PubMed: 15624019]

28. Altomare DA, Testa JR. Perturbations of the AKT signaling pathway in human cancer. Oncogene 2005;24(50):7455–7464. [PubMed: 16288292]
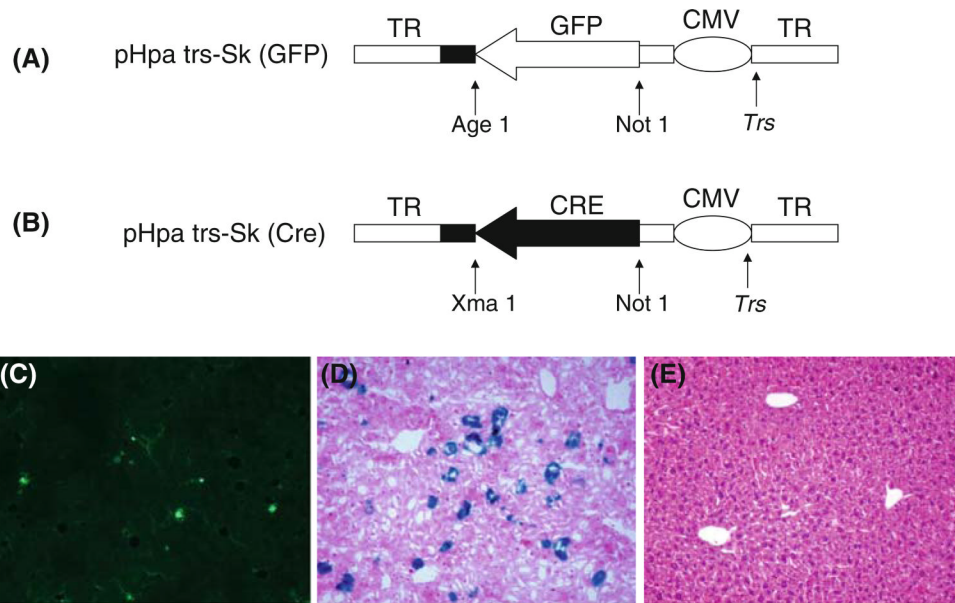
Fig. 1.
Generation of the scAAV-Cre vector and hepatocyte's transduction. **a** pHpa-trs-SK plasmid carrying GFP (scAAV-GFP); **b** scAAV-CRE, GFP was excised from the pHpa-trs-SK plasmid and Cre substituted for GFP; **c** Reporter gene expression in the liver 4 weeks after scAAV-GFP injected; **d** Frozen liver section X-gal stain 4 weeks after the scAAV-Cre vector injected into ROSA26 reporter mice showing diffuse β-galactosidase positive hepatocytes, expression of β-galactosidase indicated Cre-mediated excision of the loxP flanked stop signal and hepatocytes have undergone Cre-mediated recombination; **e** H&E stain showed no inflammatory cell infiltration in livers from scAAV-Cre injected mice. Magnification, ×100 (**c** through **e**)
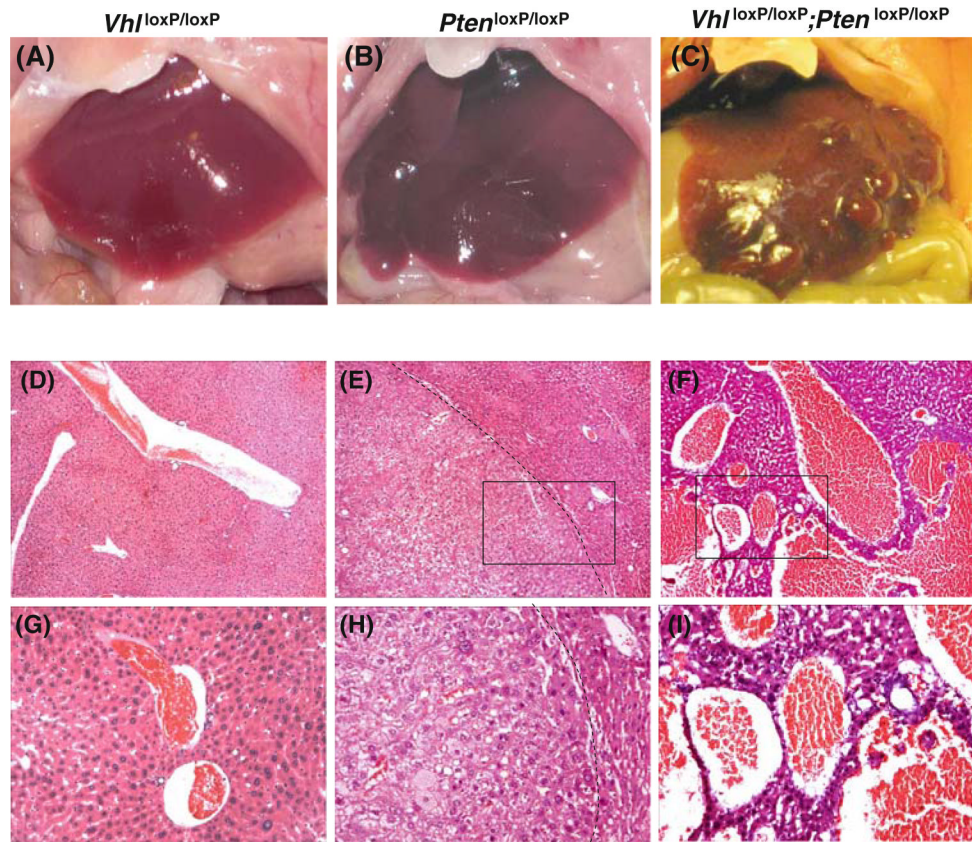
Fig. 2.
Comparison of external morphology and histological appearance of livers from AAV-Cre vector injected $Vhl^{\text{loxP/loxP}}$ (**a, d, g**), $Pten^{\text{loxP/loxP}}$ (*b, e, h*), and $Vhl^{\text{loxP/loxP}};Pten^{\text{loxP/loxP}}$ (**c, f, i**) mice. On gross examination, livers from AAV-Cre vector injected $Vhl^{\text{loxP/loxP}}$ (**a**), $Pten^{\text{loxP/loxP}}$ (**b**) appeared normal; livers from $Vhl^{\text{loxP/loxP}};Pten^{\text{loxP/loxP}}$ mice (**c**) showed irregular shape and multiple vascular lesions. Magnification, ×40 (**d–f**), ×100 (**g–i**)
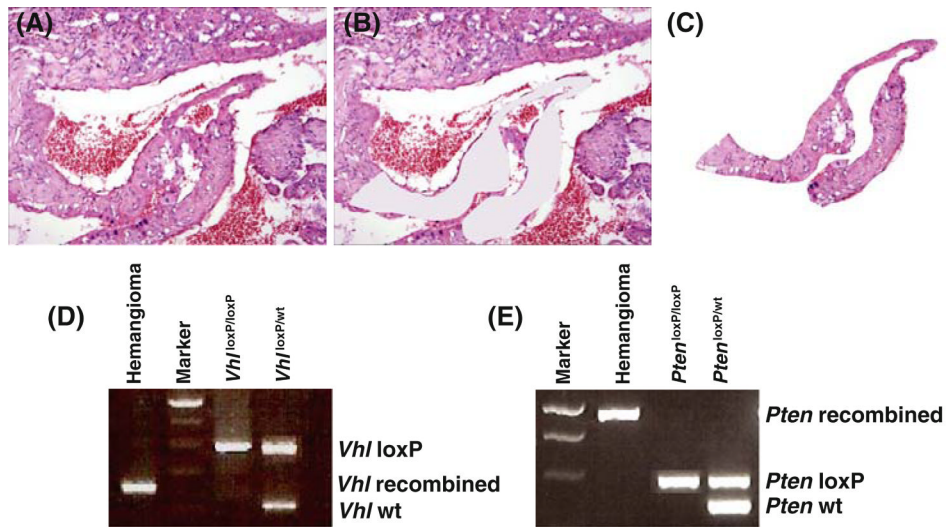
Fig. 3.
The highly vascular liver lesions from a $Vhl^{loxP/loxP};Pten^{loxP/loxP}$ mouse were isolated by using LCM. PCR analysis of recombination at the Vhl and $Pten$ loci in the mice with recombination of AAV-Cre vector, showing Vhl and $Pten$ floxed, recombined, and wild type alleles, respectively. (**a**) before dissection; (**b**) after dissection; (**c**) dissected tissue; (**d**) Vhl; (**e**) $Pten$
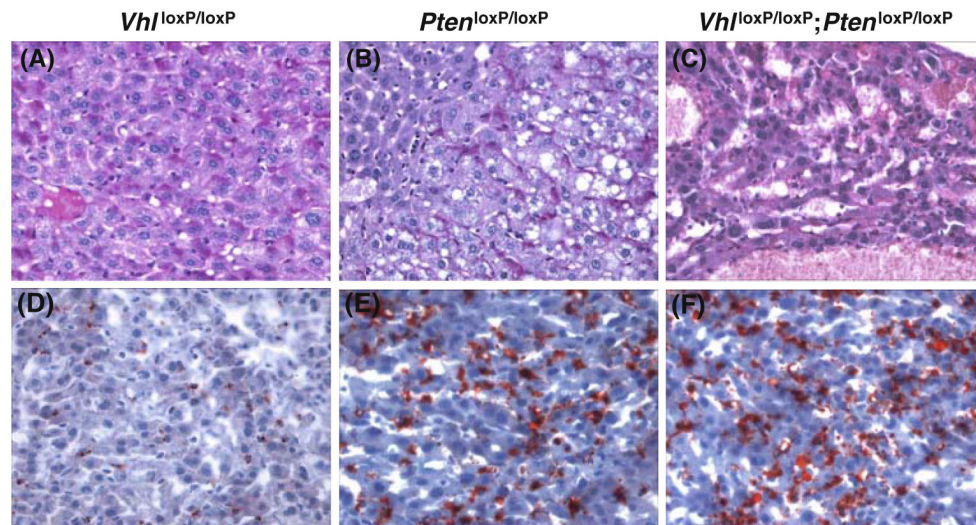
Fig. 4.
PAS (**a–c**) and *oil red O stain* (**d–f**) of livers from AAV-Cre vector injected *Vhl* $^{loxP/loxP}$ (**a, d**), *Pten* $^{loxP/loxP}$ (**b, e**), and *Vhl*$^{loxP/loxP}$;*Pten* $^{loxP/loxP}$ (**c, f**) mice demonstrate the presence of glycogen (*PAS*) or lipid (*oil red O stain*). Magnification, ×200 (**a** through **e**) (Color figure online)
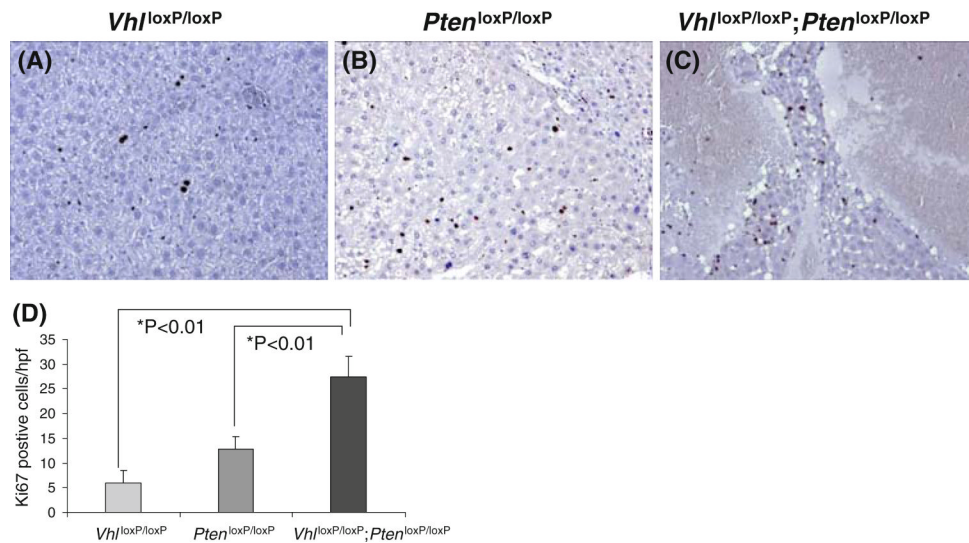
Fig. 5.
Immunohistochemical analysis of livers from $Vhl^{loxP/loxP}$ (**a**), $Pten^{loxP/loxP}$ (**b**), and $Vhl^{loxP/loxP};Pten^{loxP/loxP}$ (**c**) mice using an antibody against the proliferation marker Ki-67. **d** Quantification of the number of positive cells per high power field of the liver (×400). One field per liver section was counted and the data represent mean ± standard deviation. * Statistically significant difference between $Vhl^{loxP/loxP};Pten^{loxP/loxP}$ and all other genotypes ($P < 0.01$, student's t test). Magnification, ×200 (**a** through **c**)
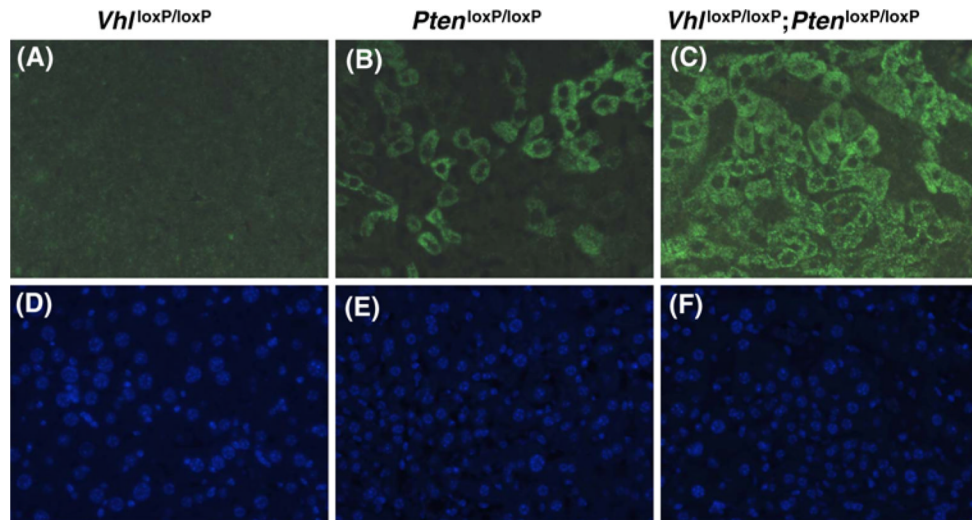
Fig. 6.
Immunohistochemical analysis of livers from AAV-Cre vector injected $Vhl^{loxP/loxP}$ (**a**), $Pten^{loxP/loxP}$ (**b**), and $Vhl^{loxP/loxP};Pten^{loxP/loxP}$ (**c**) mice using an antibody against the phosphorylated AKT. Panel b showed that phosphorylated AKT was sporadically positive in livers from $Pten^{loxP/loxP}$ mice; Panel c showed phosphorylated AKT presence in hepatocytes around the vascular lesions in $Vhl^{loxP/loxP};Pten^{loxP/loxP}$ mice. Magnification, ×200 (**a** through **c**)
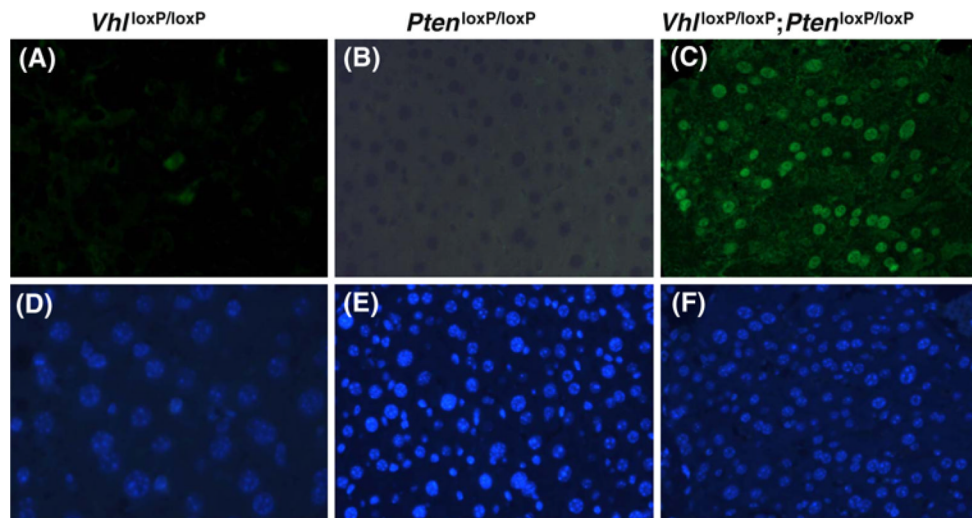
Fig. 7.
Immunohistochemistry stain of HIF-1α in livers from AAV-Cre vector injected $Vhl^{\text{loxP/loxP}}$ (**a, d**), $Pten^{\text{loxP/loxP}}$ (**b, e**), and $Vhl^{\text{loxP/loxP}};Pten^{\text{loxP/loxP}}$ (**c, f**) mice. Panel c showed HIF-1α expression upregulated in livers from $Vhl^{\text{loxP/loxP}};Pten^{\text{loxP/loxP}}$ mice. **d–f** showed the corresponding nuclear DAPI stain. Magnification, $\times$200 (**a** through **f**)
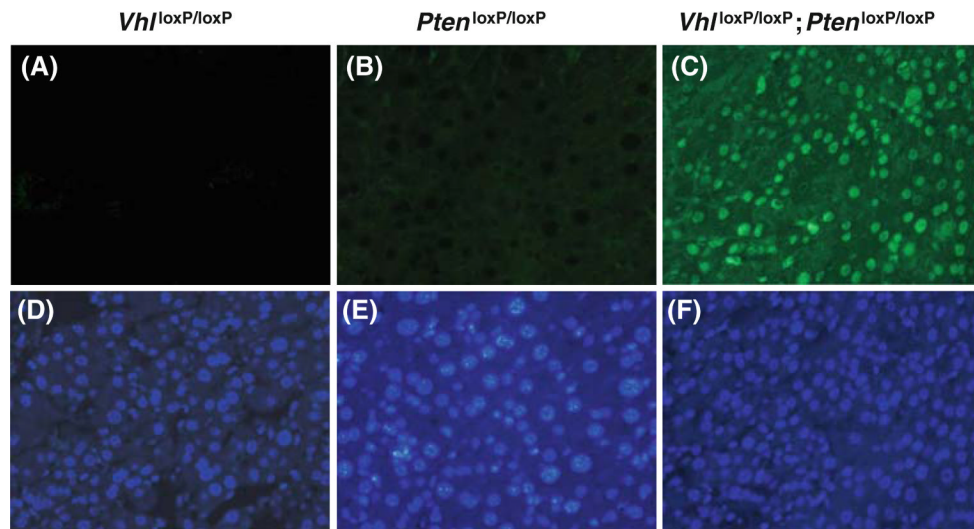
Fig. 8.
Immunohistochemistry stain of HIF-2α in livers from AAV-Cre vector injected $Vhl^{loxP/loxP}$ (**a, d**), $Pten^{loxP/loxP}$ (**b, e**), and $Vhl^{loxP/loxP}$;$Pten^{loxP/loxP}$ (**c, f**) mice. Panel c showed HIF-2α expression upregulated in livers from $Vhl^{loxP/loxP}$;$Pten^{loxP/loxP}$ mice. **d–f** showed the corresponding nuclear DAPI stain. Magnification, ×200 (**a** through **f**)
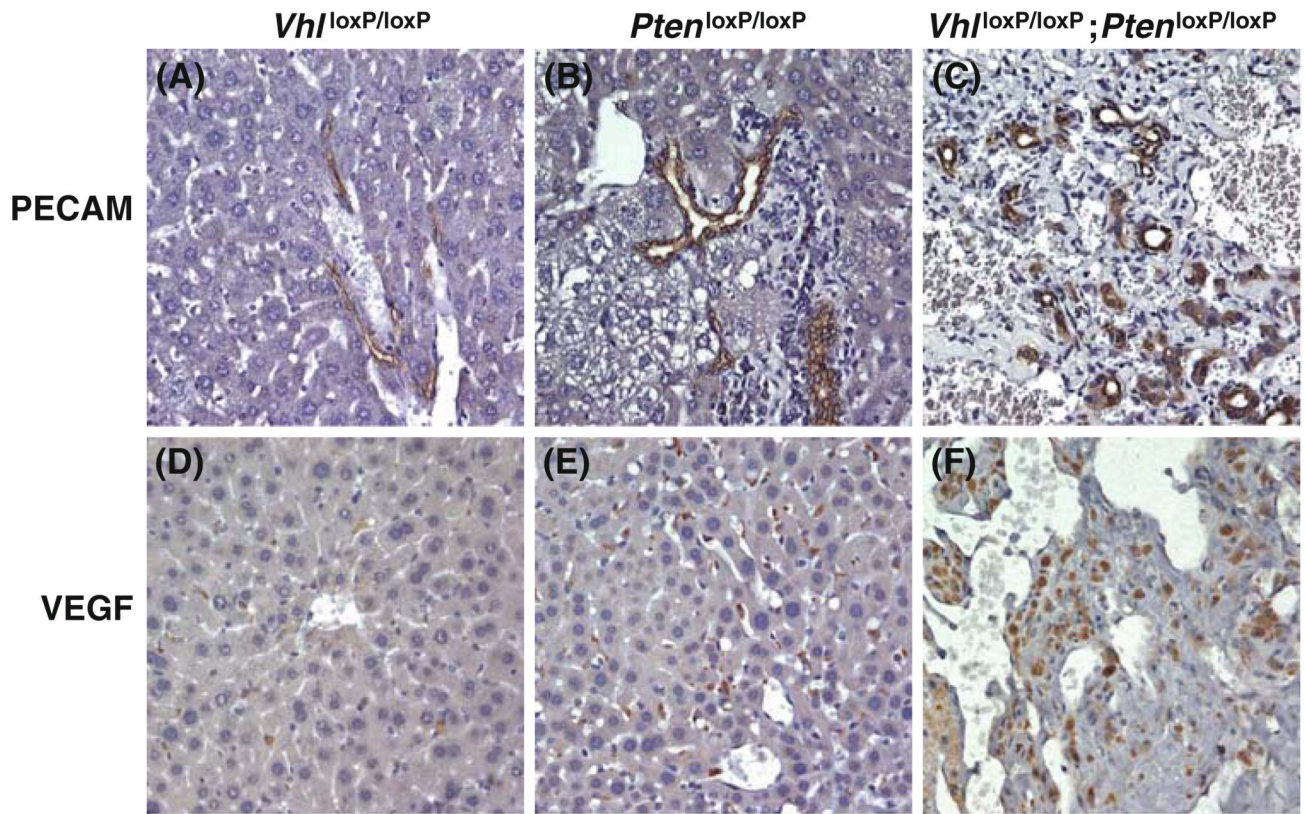
Fig. 9.
Immunohistochemistry stain of PECAM and VEGF in livers from AAV-Cre vector injected $Vhl^{loxP/loxP}$ (**a, d**), $Pten^{loxP/loxP}$ (**b, e**), and $Vhl^{loxP/loxP};Pten^{loxP/loxP}$ (**c, f**) mice. **c** PECAM expression upregulated in the liver vascular lesions from $Vhl^{loxP/loxP};Pten^{loxP/loxP}$ mice. **f** VEGF expression upregulated in the liver vascular lesions from $Vhl^{loxP/loxP};Pten^{loxP/loxP}$ mice. Magnification, ×200 (**a** through **f**)

Table 1

Occurrence of liver pathology in conditional mutant mice

Genotyping	No. of mice with described lesions	Histopathology pathology	Latency (months)
Pten loxP/loxP	18/20	Hepatocyte lipid	9
Pten loxP/loxP	2/20	Liver tumor	9
Vhl loxP/loxP ;*Pten* loxP/loxP	13/15	Vascular lesions	9
Vhl loxP/loxP ;*Pten* loxP/loxP	2/15	Hepatocyte proliferation Basophilic cell infiltration	9